1-14-2008

# Preparation and Characterization of 3 nm Magnetic NiAu Nanoparticles

Bethany J. Auten
*Trinity University*

B. P. Hahn

G. Vijayaraghavan

K. J. Stevenson

Bert D. Chandler
*Trinity University*, bchandle@trinity.edu

# Preparation and Characterization of 3 nm Magnetic NiAu Nanoparticles

**Bethany J. Auten,[†] Benjamin P. Hahn,[‡] Ganesh Vijayaraghavan,[‡] Keith J. Stevenson,[‡] and Bert D. Chandler*,[†]**

*Department of Chemistry, Trinity University, San Antonio, Texas 78212-7200, and Department of Chemistry, University of Texas at Austin, 1 University Station A5300, Austin, Texas 78712-0165*

*Received: August 30, 2007; In Final Form: January 14, 2008*

Using PAMAM dendrimers as nanoparticle templates, a synthetic route to prepare 3 nm magnetic NiAu nanoparticles was developed. Aqueous solutions of hydroxyl-terminated generation 5 PAMAM dendrimers in 25 mM $NaClO_4$ were shown to bind aqueous $Ni^{II}$. Coreduction of $Ni^{II}$ and $Au^{III}$ salts yielded bimetallic dendrimer stabilized nanoparticles, which were extracted into toluene with decanethiol. Characterization of the resulting monolayer protected clusters (MPCs) with transmission electron microscopy and UV−visible, atomic absorption, and X-ray photoelectron spectroscopies suggested that the MPCs had substantial surface enrichment in Au. Superconducting quantum interference device (SQUID) measurements at 5 K show the bimetallic MPCs to have low coercivity and saturation magnetization relative to bulk Ni. Solution nuclear magnetic resonance (NMR) studies using the Evans method showed the bimetallic nanoparticles retain magnetic properties at ambient temperatures.

## Introduction

The wide applicability of gold nanoparticles is now universally recognized.[1] Au nanoparticle (NP) synthesis is now a relatively mature field, with synthetic routes available for the preparation of particle sizes from 1 to nearly 100 nm.[1−5] Future advances in gold nanoparticle chemistry will likely necessitate the ability to tune the properties of Au nanoparticles or add new functionality to predominantly Au nanoparticles. One potential means of accomplishing this is to incorporate heterometals, particularly inexpensive first row transition metals, into Au NPs.

Imparting magnetic properties to predominately Au nanoparticles motivates their use in a number of potential biomedical applications, particularly as MRI contrast or enhancement agents,[6−8] as labels for DNA[9,10] or cancer cells,[11] and as chromatography agents in biomolecular separations.[12,13] Because magnetic elements such as Co, Fe, and Ni are potentially toxic, bimetallic particles may need to have core−shell morphologies with predominately Au surfaces to be used in these systems.[14] The rich chemistry of the high affinity between gold and sulfur-containing ligands also gives Au shell materials several potential advantages in tailoring particles for specific applications.[14] However, preparing monodisperse nanoparticles in the functional size regime (<20 nm) remains a substantial challenge for the aforementioned applications[13−15] and there are exceedingly few reports of bimetallic magnetic nanoparticles smaller than 5 nm in the literature.[16]

PAMAM dendrimer encapsulated nanoparticles (DENs) and dendrimer stabilized nanoparticles (DSNs) offer a new synthetic route to bimetallic nanomaterials.[5,17] The dendrimer templating method provides substantial flexibility for adapting syntheses to a variety of transition metals and can be employed using either organic or aqueous solvents.[5,17] Crooks and co-workers recently reported on the synthesis and magnetic properties of <2 nm Ni DENs,[16] and a number of papers from this group have developed synthetic methodologies for preparing Au and bimetallic Au−M DENs.[18−23] In developing these preparative methods, they have additionally shown that Au, Ag, and Pd mono- and bimetallic nanoparticles can be extracted from aqueous DENs into organic solvents using appropriate alkanethiols or carboxylic acids.[18,22,23] The resulting monolayer protected clusters (MPCs) are structurally similar to those prepared via the Brust−Schiffrin method[2,3] but have well-defined stoichiometries arising from the dendrimer templating process.

Bimetallic NiAu NPs have the potential to impact a variety of fields; however, the dearth of synthetic routes for preparing NiAu nanoparticles has prevented the exploration of this binary system. For example, computational[24] and surface science[25,26] studies of NiAu surface alloys indicate promise for advances in heterogeneous catalysts. However, Ni and Au are essentially immiscible at room temperature as the bulk phase diagram has a broad miscibility gap between 5 and 99% Au.[27] This bulk instability, which leads to rapid phase segregation, has made the synthesis of NiAu nanoparticles and catalysts a substantial synthetic challenge. Standard impregnation techniques lead 50+ nm particles and minimal interaction between the two metals.[28] Attempts have also been made to reduce Au onto Ni particles anchored onto an oxide support; however, this results in only the decoration of some Ni particles and the preparation of large (10−20 nm) Au particles.[29,30] Other reports of NiAu NPs similarly involve methods that are not readily adapted to the preparation of soluble NPs from Ni and Au salts, such as X-ray induced reduction with a synchrotron source[31] or chemical reduction in a gellike host matrix such as gelatin.[32]

Our interests have been in the controlled preparation of bimetallic nanoparticles and catalysts, particularly for synthetically challenging metal systems. We have previously employed PAMAM dendrimers in the preparation of bimetallic PtAu

* To whom correspondence should be addressed: Phone: (210) 999-7557. Fax: (210) 999-7569. E-mail: Bert.chandler@trinity.edu.
[†] Trinity University.
[‡] University of Texas at Austin.

10.1021/jp076982c CCC: $40.75 
Published on Web 03/19/2008

particles, which also have a wide bulk miscibility gap.[33] In this study, we report the application of the dendrimer templating and thiol extraction synthetic techniques to the tailored synthesis of 3 nm NiAu NPs functionalized with decanethiol. NiAu NPs have potential applications in a variety of biomedical areas, particularly where surface functionalization chemistries are important, so the magnetic properties of these new materials were also reported.

## Experimental Section

**Materials.** Nanoparticle (NP) synthesis was performed in nanopure water. Fifth generation hydroxyl-terminated Starburst PAMAM dendrimers (G5-OH) were obtained from Dendritech as a 23% methanolic solution. Prior to use, methanol was removed by rotary evaporation at room temperature. $Ni(NO_3)_2 \cdot 6H_2O$, $NaBH_4$, $NaClO_4$, and $C_{10}H_{22}S$ were purchased from Aldrich. $HAuCl_4$ was obtained from Strem Chemicals, and toluene and ethanol (200 proof) were from Fisher Chemicals. All reagents were used without further purification.

**Synthesis of Au DSNs.** Au dendrimer stabilized nanoparticles (DSNs) were prepared under $N_2$ on the basis of the literature procedure.[18] $NaClO_4$ (200 $\mu$L, 1 M) was first added to an aqueous solution of G5-OH PAMAM dendrimers (5 mL, 9.75 $\mu$M). Au NPs were then prepared by adding $AuCl_4^-$ (2.25 mL, 3.25 mM, 150 equiv of Au/G5-OH) to the dendrimer solution and stirring for 2 min. $NaBH_4$ (0.1 M, 1.7 mL) in NaOH (0.1 M) was then added causing an instantaneous color change from pale yellow to brown. The solution was allowed to stir for 15 min after reduction.

**Synthesis of NiAu DSNs.** Ni−Au DSNs were similarly prepared under $N_2$ with a Ni:Au:Dendrimer ratio of 55:110:1, respectively. $Ni(NO_3)_2 \cdot 6H_2O$ (90 $\mu$L, 30 mM) was stirred with the G5-OH PAMAM dendrimer (5 mL, 9.75 $\mu$M) + $NaClO_4$ (200 $\mu$L, 1 M) solution for 20 min before $HAuCl_4$ (1.70 mL, 3.25 mM) was added. After 2 min of stirring, $NaBH_4$ (0.1 M, 1.7 mL) in 0.1 M NaOH was added. The solution turned brown upon addition of the reductant but was allowed to stir for 15 min.

**Extraction of Ni−Au NPs from Dendrimer Template.** Extraction of NiAu NPs was accomplished by following a previously described procedure[19] Briefly, 100 equiv of solid $NaBH_4$ was added to the DSN solution. The DSNs were then extracted from the aqueous layer using a freshly prepared and degassed solution of 1-decanethiol in toluene (0.1 M, 8 mL). The layers were shaken in a separatory funnel for 5 min and allowed to settle for 5 min before separation. A small amount of brown precipitate was also formed.[34]

The isolated Ni−Au MPCs were purified by a precipitation protocol outlined by Crooks and co-workers.[35] The organic layer was concentrated to 1 mL by rotary evaporation. Ethanol (15 mL) was added to the 1 mL Au NP toluene solution and centrifuged for 20 min. The precipitate was then collected and redissolved in 1 mL of toluene, and the purification was repeated. After the second collection of the solid, the NPs were redissolved in 1 mL of toluene and dried completely by rotary evaporation.

**UV−Visible and Atomic Absorption Spectroscopy.** Solution UV−visible absorbance spectra were collected on a Jasco V-530 spectrometer using quartz cells and toluene or water as the reference. Gold and nickel elemental concentrations were determined with a Varian SpectrAA 220FS using an acetylene/air flame.[36] Samples were placed in an Erlenmeyer flask and prepared for AA studies by evaporating the toluene in a sand bath overnight. Erlenmeyer flasks were then placed in a muffle furnace for 1 h at 250 °C to remove the thiol. Freshly prepared aqua regia (3 mL) was then added to the sample and allowed to digest at room temperature for 30 min. The sample was then heated slowly to 60 °C for 2 h. The sample was transferred to a volumetric flask (10 mL), and $NH_4OH$ (3.7 N) was added dropwise until neutralized. The sample was diluted to mark with nanopure water and subsequently analyzed.

**Transmission Electron Microscopy (TEM).** Transmission electron microscopy (TEM) was performed with a JEOL 2010F microscope operating at 200 kV. Nanoparticles suspended in hexane were drop cast onto a 150 mesh Cu TEM grid covered with a thin amorphous carbon film. Image analysis was performed with DigitalMicrograph 3.6.1 (Gatan) software. Particle size distributions were determined with ImageJ software using the perimeter and area of at least 90 particles for each sample.

**X-ray Photoelectron Spectroscopy (XPS).** XPS measurements were collected with a Kratos Axis Ultra X-ray photoelectron spectrometer using an unmonochromated Al K$\alpha$ source. This instrument was calibrated against adventitious carbon using the C 1s line at 285.0 eV.[37] Survey scans were acquired of all materials with high-resolution scans of the Au 4f, Ni 2p, and S 2p electronic transitions. The XPS peaks obtained were deconvoluted and fitted with the freeware FITT program (version 1.2, written by Hyun-Jo Kim) using a modified Levenberg−Marquardt peak fit[38] The Shirley method was used for all background corrections.[39]

**Superconducting Quantum Interference Device (SQUID) Magnetometer Studies.** SQUID measurements were carried out using a Quantum Model Design MPMS SQUID magnetometer. Samples of ~25.7 mg were prepared by combining multiple batches of NiAu MPCs. After reduction of the volume with rotary evapoartion, the thick tarlike sample was transferred into the SQUID capsule. Hysteresis curves at 5 K were measured over magnetic field strengths of −50 to +50 kOe; magnetization vs temperature curves were collected from 5 to 273 K.

**Evans Method.** $^1$H NMR spectra were recorded on a Varian Unity/Inova 400 spectrometer at an operating frequency of 399.96 MHz. The $^1$H chemical shifts were referenced to internal solvent peaks. Prior to characterization, the aqueous NP solutions were purified twice by precipitation in ethanol, dried by rotary evaporation, and redissolved in toluene-$d_8$ (0.60 mL). A capillary tube containing toluene-$d_8$ was suspended in the middle of the NMR tube containing the sample. Au MPCs: $H^1$ NMR (400 MHz, $C_6D_5CD_3$) $\delta$ 2.06 ppm ($C_6H_5CH_3$) for the capillary and sample. NiAu MPCs: $H^1$ NMR (400 MHz, $CDCl_3$) $\delta$ 2.06 ppm ($C_6H_5CH_3$) for the capillary and 2.07 ppm ($C_6H_5CH_3$) for the sample.

## Results and Discussion

**Effects of Ionic Strength on DSN Synthesis.** Crooks' group initially reported the preparation of water soluble Au DENs,[20] and they have subsequently shown that Au nanoparticles can be extracted from PAMAM dendrimer interiors with alkanethiols.[18] Additionally, PAMAM dendrimers modified with alkyl chains have been used to bind $Ni^{II}$ salts from dilute organic solution and can be used to prepare monometallic magnetic nanoparticles in toluene.[16] However, we are unaware of previous studies reporting $Ni^{II}$ binding by hydroxyl-terminated PAMAM dendrimers in water.

Figure 1 shows the UV−visible spectrum of $Ni^{II}$ (3.3 mM) in water with the diagnostic split band at 650 and 700 nm. This splitting is due to spin−orbit coupling that mixes the $^3T_{1g}(F)$ and $^1E_g$ states, which are very close in energy at the ligand field

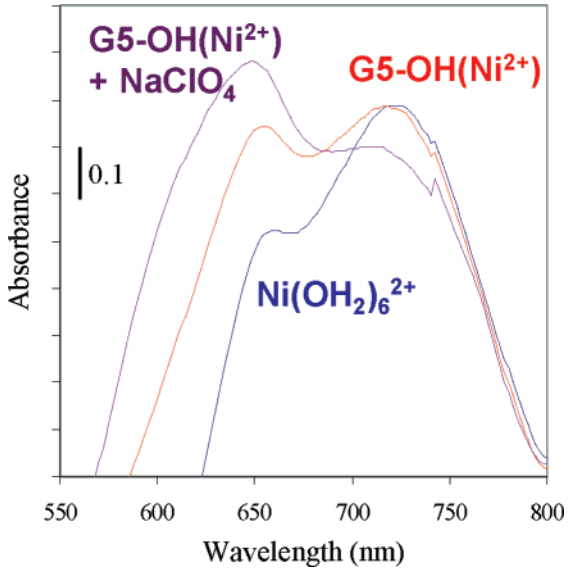


**Figure 1.** UV−vis spectra of Ni binding studies.

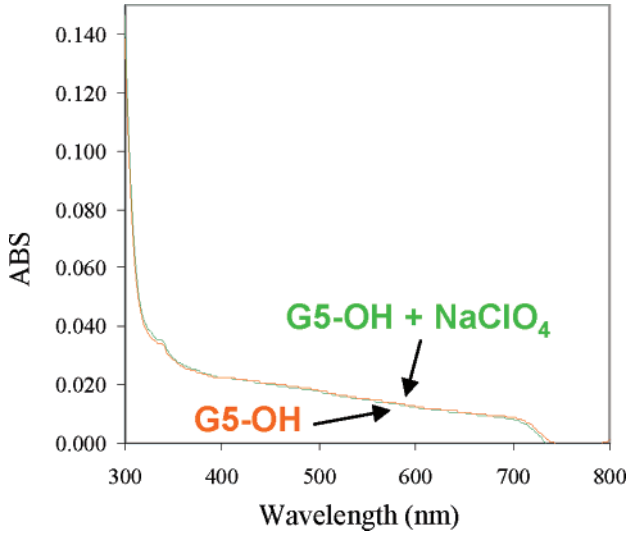


**Figure 2.** UV−vis spectra of $NaClO_4$ effects on G5-OH.

splitting ($\Delta_O$) value given by six water ligands.[40] The addition of $Ni^{II}$ to G5-OH resulted in a blue shift of approximately 5 nm in the higher energy shoulder of the split band, suggesting a minor or partial change in the nickel coordination sphere. $Ni^{II}$ readily binds ethylene diamine in aqueous solution,[40] so it is surprising that G5-OH does not readily bind $Ni^{II}$ (the small shift and overlapping peaks suggests that the ligand exchange may not be quantitative under these conditions). It seemed plausible that the transition metal was not able to access the dendrimer interior, so we attempted to affect the exterior branches of the dendrimer by increasing the solution ionic strength.

As shown in Figure 1, the $Ni^{II}$ spectrum blue shifts further in the presence of 25 mM $NaClO_4$. There is an additional 5 nm blue shift in the higher energy portion of the split band and a corresponding reduction in the longer wavelength portion of the band. These changes are consistent with the addition of stronger field ligands to the $Ni^{II}$ coordination sphere[40] and indicate displacement of $H_2O$ molecules by interior amines and/or amides in the dendrimer. The change also suggests that increasing the solution ionic strength helps to open the dendrimer, providing $Ni^{II}$ ions with greater access to the dendrimer interior. This increase in ionic strength did not affect the UV−visible spectrum of the dendrimer containing no $Ni^{II}$ (Figure 2).

Because increasing the solution ionic strength enhances the dendrimer's ability to bind $Ni^{II}$, it may also affect the dendrimer's ability to stabilize nanoparticles. To evaluate the effects of solution ionic strength on the stability of dendrimer templated nanoparticles, we prepared a series of G5-OH($Au_n$) DENs ($n$ = 50, 150, 200, and 250) and monitored the UV−visible spectra after increasing the ionic strength of the solution to 100 mM $NaClO_4$ (see Supporting Information). The $Au_{50}$ and $Au_{150}$ DEN solutions showed no substantial changes over several days in the higher ionic strength solution. For DENs larger than $Au_{150}$, the increase in ionic strength caused rapid precipitation of the nanoparticles and a concomitant reduction in the solution plasmon band. Thus, high ionic strength solutions reduce the dendrimer's ability to solubilize nanoparticles, particularly for large metal:dendrimer stoichiometries. Under the conditions used in the synthesis of NiAu MPCs below, the solution ionic strength (which is required for $Ni^{II}$ binding by G5-OH) had no observable affect on nanoparticle stability.

**Synthesis and Characterization of NiAu MPCs.** With the above experimental parameters in mind, the synthesis for alkanethiol-stabilized Au MPCs was tailored for the preparation of bimetallic NiAu nanoparticles. Aqueous solutions of $Ni(NO_3)_2 \cdot 6H_2O$ (55 equiv) and $HAuCl_4$ (113 equiv) were sequentially added to G5-OH PAMAM dendrimers in a 25 mM $NaClO_4$ solution. Addition of $NaBH_4$ instantly turned the solution from pale yellow to dark brown. After exposure to borohydride for 20 min, the NiAu nanoparticles were transferred to a separatory funnel and extracted with an equivalent volume of 0.1 M decanethiol in toluene. The potential long-term instability of the nanoparticles in the higher ionic strength solution necessitated rapid extraction of the nanoparticles as monolayer protected clusters (MPCs), and precluded complete characterization of the dendrimer−nanoparticle composites. Because these intermediate species have not been fully characterized, we conservatively refer to them as dendrimer stabilized nanoparticles (DSNs) rather than dendrimer-encapsulated nanoparticles (DENs) as we cannot readily determine how much metal, if any, resides outside of the dendrimer cavity.

Figure 3 shows UV−visible spectra of the Au and NiAu DSNs and MPCs prepared from 25 mM $NaClO_4$ solutions of G5-OH. The Au MPC sample shows a weak absorbance at 525 nm, characteristic of the Mie plasmon band for Au nanoparticles smaller than 3 nm. This shoulder at 525 nm is also present in the NiAu MPCs but is markedly less pronounced. For both samples, the plasmon band is slightly more pronounced after extraction. Previous work by Crooks' group has attributed similar enhancement to charging of the plasmon band by the borohydride reducing agent,[41] and it may also indicate a small degree of particle agglomeration during extraction. Monometallic Ni samples used as controls could not be extracted from water into toluene using comparable procedures and conditions.

The extracted bimetallic MPCs, which are the focus of the remainder of this study, were stable for weeks when stored at room temperature under nitrogen. They showed no change in their UV−visible spectrum beyond a small amount of initial precipitation (see Supporting Information). The experimentally determined Au:Ni atomic ratio, measured with atomic absorption spectroscopy, was 2.1 ± 0.3 (see Supporting Information). This value is nearly identical with the expected Au:Ni ratio of 2.05 on the basis of the synthetic conditions and is in the immiscible region of the bulk Ni−Au phase diagram.[27]

Figure 4 shows TEM micrographs and particle size distributions for Au and NiAu MPCs. Particles sizes for both samples are essentially the same with the average diameters being 2.9

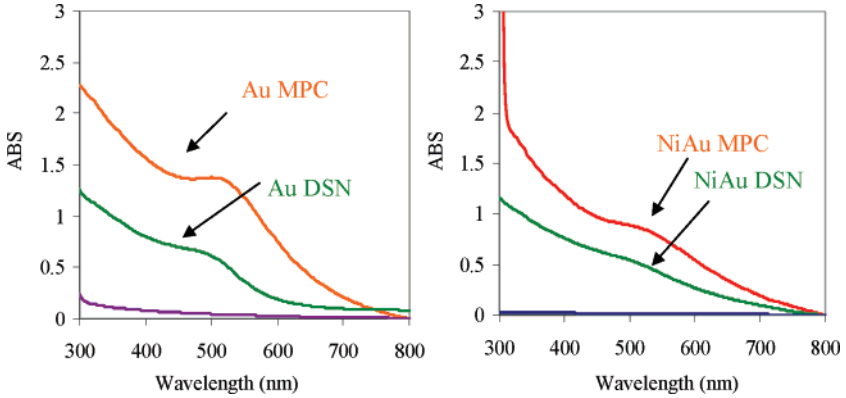


**Figure 3.** UV−vis of Au and Au−Ni DSN and MPC.

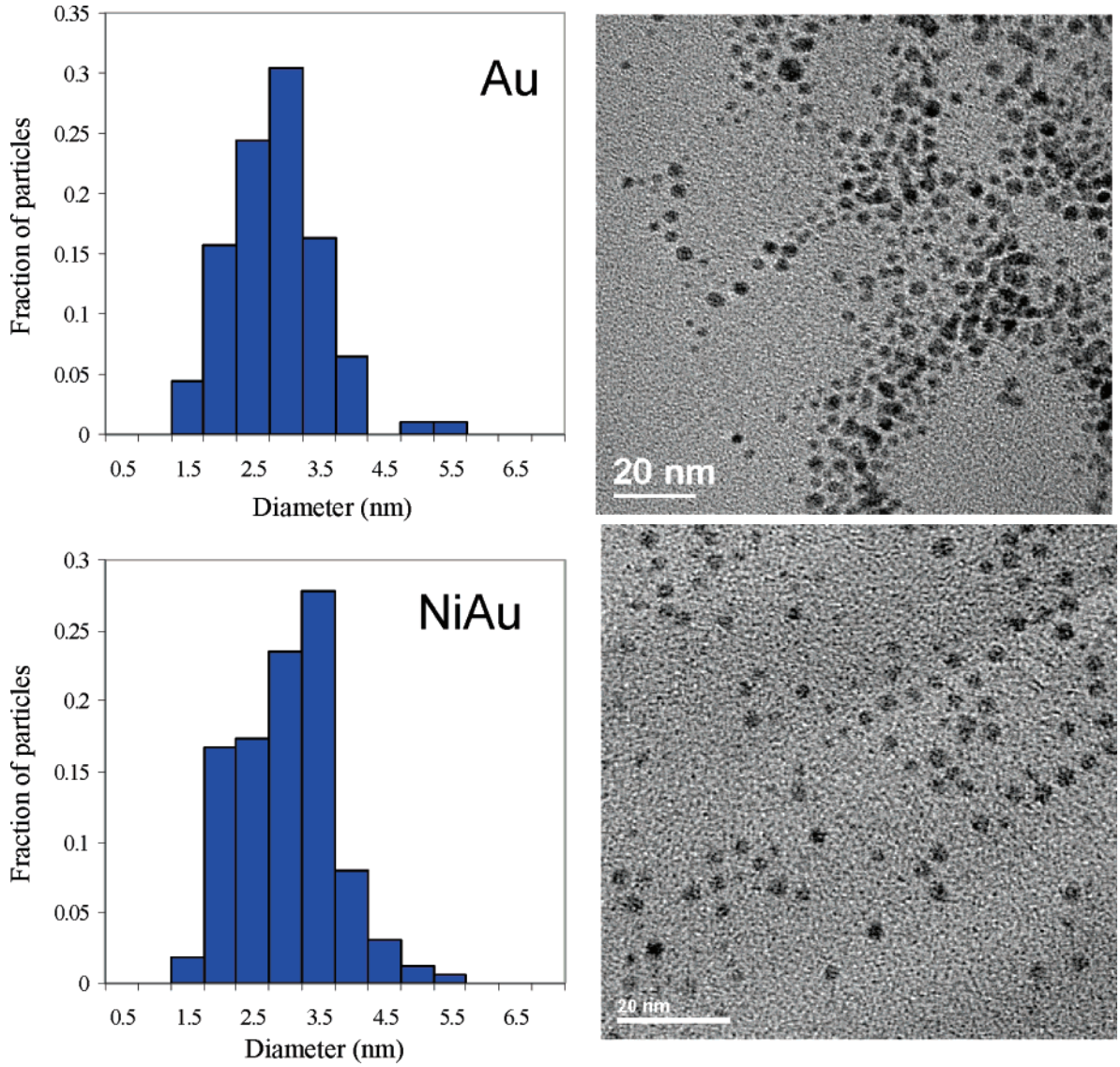


**Figure 4.** TEM micrographs of Au and Au−Ni MPCs.

± 0.7 nm (Au MPCs) and 3.0 ± 0.8 nm (NiAu MPCs). The extracted particles are slightly larger than expected sizes on the basis of the initial synthetic conditions (ca. 2 nm). On the basis of the UV−vis data (vide supra), this particle growth likely occurs during the extraction into the organic solvent. Energy dispersive spectroscopy (EDS) spectra were recorded for several single particles, but the Ni signal was too weak to separate from the intense Cu signal arising from the TEM grids. EDS spectra of larger regions containing approximately 10 particles (see Supporting Information) provided sufficient signal to confirm the presence of both Ni and Au. The EDS data showed particles slightly enriched in Au (80%) relative to the bulk measurements, indicating that there is likely a distribution of particle compositions.

X-ray photoelectron spectroscopy (XPS) studies were performed on the Au and NiAu MPCs and are shown in Figures 5 and 6. The sulfur 2p peak for both the Au and NiAu MPCs was found at 164 eV, similar to bulk S. For the Au MPCs, the

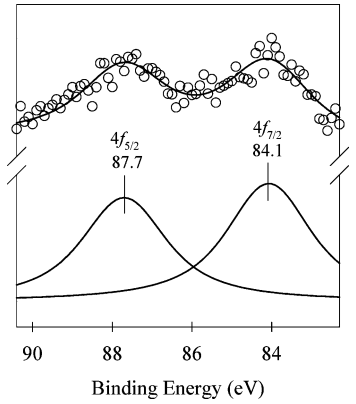


**Figure 5.** XPS of Au MPCs.

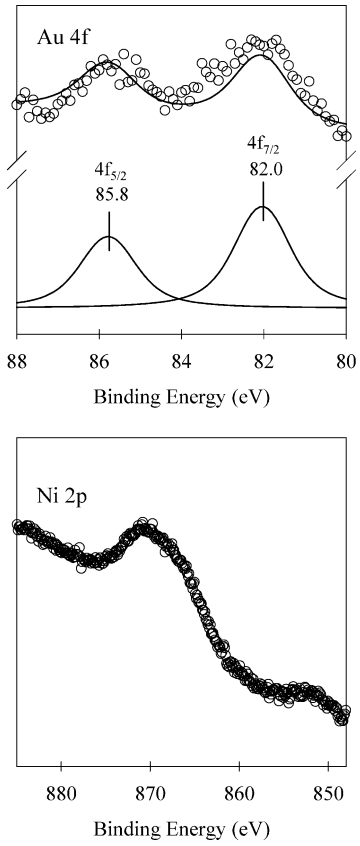


**Figure 6.** XPS of Au−Ni MPCs.

Au 4f peaks had energies of 84.1 and 87.7 eV, which are slightly shifted from bulk Au. Similar shifts in the Au 4f peaks in Au NPs have been reported in the literature and attributed to the accumulation of positive charge on surface Au atoms due to the Au−S bonds on the MPC surface.[42,43]

Relative to the Au MPCs, the Au 4f electrons in the XPS spectrum of the NiAu MPCs are shifted approximately 2 eV toward lower binding energy. Brayner et al. reported a similar Au 4f region with some lower energy peaks for gelatin immobilized 12−20 nm NiAu NPs.[32] The shift we observe is consistent with the incorporation of electron-donating materials into the Au nanoparticle, although the magnitude of the shift is probably larger than can be attributed to electron donation from metallic nickel alone. It is likely that some boride (or possibly some trapped hydride) is incorporated into the nanoparticle during the reduction with borohydride. The reduction of Ni salts with borohydride has been shown to produce Ni, $Ni_2B$, or mixed Ni−NiB materials, depending on the reduction conditions.[44] The presence of boron can only be inferred, however, because the B 1s peak at 191 eV typically has very low intensity[44] and was not observed in the XPS spectrum of the NiAu MPCs. Similarly, the oxidation state(s) of the Ni could not be readily determined. The Ni 2p region of the NiAu MPCs shows two broad peaks at approximately 853 and 870 eV, which indicate the presence of Ni and suggest a distribution of Ni oxidation states. Substantially larger satellite peaks convolute the $2p_{1/2}$ feature, however, and prevent us from obtaining a meaningful curve fit to the data. Nonetheless, contributions from a mixed Ni−NiB particle is consistent with the all of the XPS data (shifted Au peaks and broad Ni data).

The morphology (well-mixed vs core@shell structures) of the bimetallic particles is of particular interest. The NiAu system was chosen on the basis of three properties that bias the system toward the formation of Ni@Au core−shell nanoparticles. Ni was chosen from the group of inexpensive first row magnetic elements on the basis of its potential for forming metal-dendrimer complexes. Second, Au has the lower work function of the two metals, making it thermodynamically more stable on the particle surface. This property is enhanced by the use of alkanethiols to extract the NPs into organic solution, since the strong Au−S interactions provide additional driving force to bring Au to the NP surface. For comparison, XPS data on larger (12−20 nm) NiAu particles also showed significant surface enrichment in Au, even in the absence of thiol ligands.[32] Thus, the synthetic procedure used for the NiAu MPCs (particularly the extraction and appropriate choice or Ni:Au stoichiometry) helps to reinforce a system that is already biased toward the formation of core−shell nanoparticles.

The UV−visible data and the inability to extract monometallic Ni particles alkanethiols support the conclusion that the NiAu MPCs have surfaces that are greatly enriched in Au and, therefore, cores that are enriched in Ni. Well-mixed PtAu[33] and PdAu[21] DENs show no plasmon absorbance near 550 nm. However, Scott et al. showed that the Au plasmon band appears in core−shell nanoparticles after approximately 2 atomic layers of Au are deposited onto $Pd_{55}$ DENs.[21] They further used the appearance of the plasmon band and their synthetic methodology as the primary evidence for the preparation of core−shell nanoparticles on this length scale. Halas and co-workers have also shown that that a contiguous Au layer or shell is required for the generation of the surface plasmon band.[45]

The plasmon band for the NiAu MPCs is not present in the nascent DENs but is clearly apparent after extraction with 1-decanethiol. Some of this increase in plasmon intensity may be attributed to particle growth during extraction, but the generation of the plasmon band can only be attributed to the presence of extended Au regions in NiAu MPCs. Given the similarities to the data reported by Crooks' and Halas' groups, it is reasonable to conclude that the NiAu MPCs have substantially Au-enriched nanoparticle surfaces. Although the data indicate that the NiAu MPCs are surface-enriched in Au, we cannot comment on the thickness or completeness of the Au shell or determine if the MPCs have a true core@shell morphology.

**Magnetic Properties.** Superconducting quantum interference device (SQUID) measurements were used to quantify the magnetization of the NiAu MPCs and are shown in Figure 7. The hysteresis loop at 5 K shows the particles to have a coercitivity of 60 Oe. The saturation magnetization, determined from elemental analysis of the sample after the SQUID measurements, was found to be 10 emu/g of Ni. This value is lower than the saturation magnetization of bulk nickel (54.4

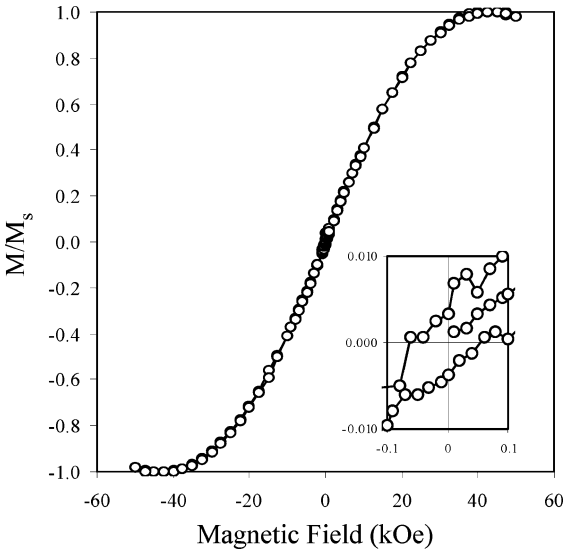


**Figure 7.** SQUID measurement of Au−Ni MPCs. The saturation magnetization was determined to be 10 emu/$g_{Ni}$.

emu/g of Ni)[46] and slightly higher than a recent value reported for Ni DENs.[16] The SQUID studies also showed the magnetization of the NiAu MPCs to become negative above 10 K. This shift, precluding a detailed examination of the temperature effects, is attributed to the large diamagnetic contribution of the alkanethiol ligands and residual solvent.

Both the lower saturation magnetization measured for the NiAu MPCs (relative to bulk Ni) and the shift to negative magnetization are consistent with a recent study from Knecht et al. on monometallic Ni DENs of 50−150 atoms.[16] Their study showed that the diamagnetic contributions of the dendrimer overwhelmed the ferromagnetic or paramagnetic contributions from the nanoparticles, even at 5 K. The precise stoichiometry between the nanoparticles and dendrimers allowed them to perform careful diamagnetic corrections using dendrimer control samples that had been treated in exactly the same fashion as the DEN but excluding the nickel. Unfortunately, comparable control experiments were not possible for the NiAu MPCs used in this study, because the NiAu nanoparticles play the central role in assembling the MPCs. Consequently, we were not able to directly monitor the changes in NiAu MPC magnetic properties above 10 K.

It is noteworthy that the NiAu MPCs show paramagnetism or weak ferromagnetism (vide infra) at 5 K where the monometallic Ni DENs were dominated by the diamagnetism of the dendrimer at this temperature. This is likely due to the smaller fraction of diamagnetic material in the MPC thiol portion relative to the large molecular weight of the PAMAM dendrimers. This may also contribute to the higher saturation magnetization observed for the NiAu MPCs relative to the Ni DENs.[16,32] As Knecht and co-workers have suggested, the presence of diamagnetic material at the particle surface may help to quench the magnetism of the surface atoms, thus reducing the observed saturation magnetization.[16] For the NiAu MPCs, which have surfaces enriched in Au, there is less diamagnetic material near the Ni atoms; i.e., a potentially protective layer of Au separates the Ni from the thiol ligands and appears to mitigate this diamagnetic quenching. It is also possible that the room-temperature paramagnetism arises largely from partially oxidized Ni−NiB regions concentrated in the nanoparticle interiors.

The ambient temperature magnetic properties of the Au and NiAu MPCs were evaluated in solution using the Evans method, which monitors a perturbation in the chemical shift of a solvent

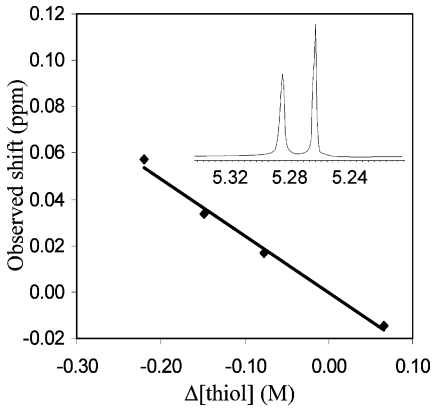


**Figure 8.** Effects of added thiol on Evan's method experiments. Changes in the chemical shift of the thiol proton of decane thiol were monitored as the concentration of the sample solution was changed. The thiol concentration in the reference tube was held constant at 0.25 M.

reference peak as a function of the magnetic environment in the sample.[47,48] Although the Evans method is experimentally straightforward, it is extremely sensitive to even small differences in the magnetic environment of the solvent in the reference and sample. Even in purely diamagnetic systems, such as the case of trace impurities of one solvent in another, the chemical shift of the impurity depends on the solvent in which it is dissolved.[49] Initial experiments with once-precipitated Au MPCs showed inconsistent apparent peak shifts between the sample and reference. After numerous control experiments, it was determined that small differences in the thiol content between the sample and the reference solution lead to an observed shift in the NMR spectrum. The control experiment shown in Figure 8 consists of a series of dummy samples with known concentrations of decanethiol in both the sample and reference. This experiment shows that the induced shifts (no nanoparticles present) decrease as the concentration of the thiol in the capillary tube approaches the concentration in the NMR tube and that the observed peak "shift" can occur in either direction depending on the differences in the thiol impurities.

The importance of eliminating all impurities necessitated more stringent sample preparation protocols to ensure that the sample and reference are as identical as possible. Evans' method experiments were therefore performed in deuterated toluene. Commercial samples contained enough proteotoluene to serve as a reasonable reference peak, thus preventing errors from adding internal standards. Additionally, MPC samples were purified by precipitating twice from toluene, with the last precipitation and final dissolution coming from deuterated toluene.

Evans' method $^1$H NMR spectra of the Au and NiAu MPCs are shown in Figure 9b,c, respectively. NMR spectra of the monometallic Au MPCs show a single methyl resonance, indicating that the purification protocol (twice precipitating and redissolving) successfully removes the excess thiol used in extracting the nanoparticles from the dendrimers.[50] The presence of monometallic Au MPCs had no effect on the toluene methyl peak in the NMR spectrum, indicating only diamagnetic behavior.

The NiAu MPCs, on the other hand, caused both a shift in the toluene methyl peak and substantial line broadening in all of the peaks in NMR spectrum. The peaks in the solvent-only monometallic Au MPCs samples show no line broadening relative to the toluene only spectrum (Figure 9a,b). The line broadening in the NiAu MPCs is likely due to the movement

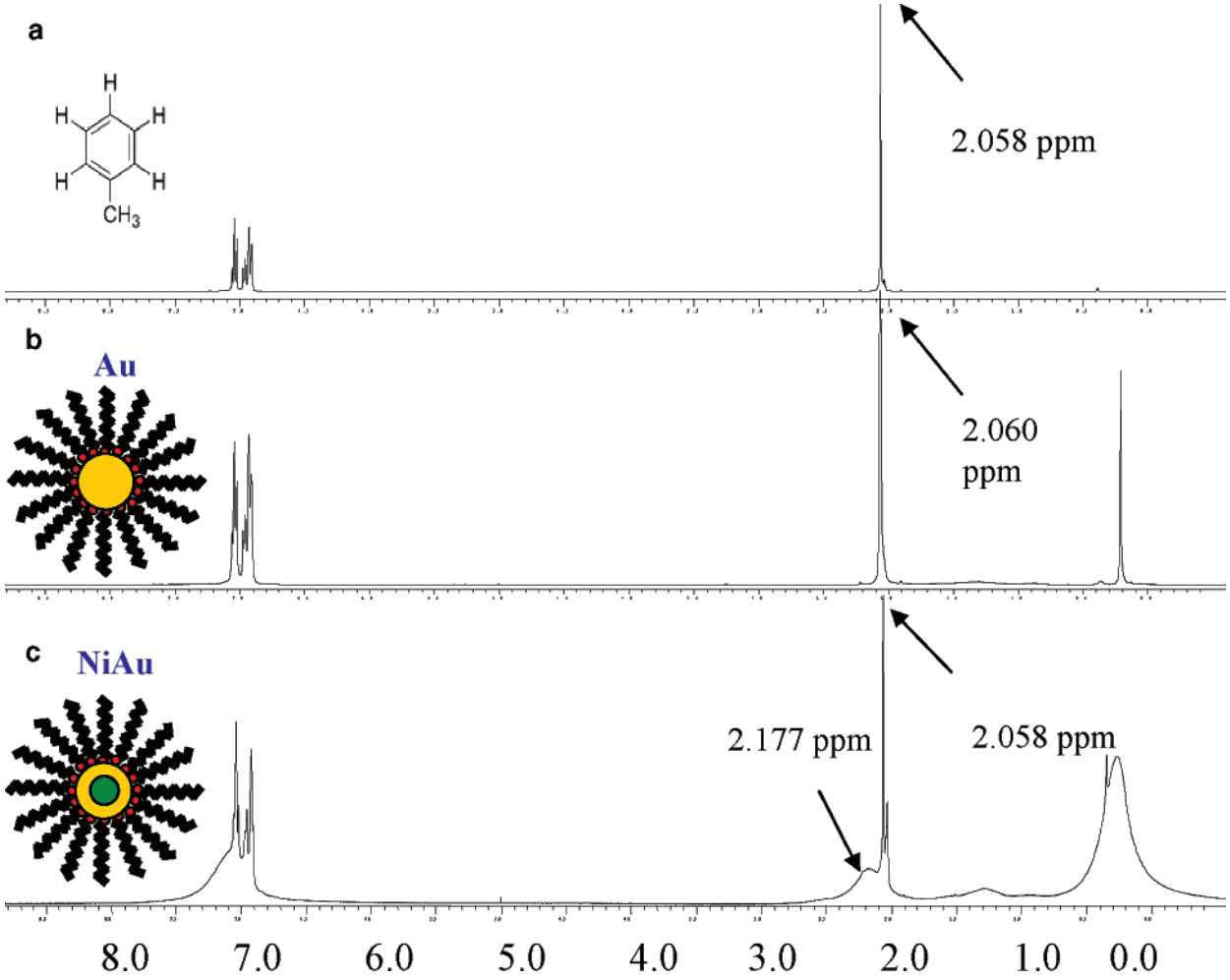


**Figure 9.** Evan's method $H^1$ NMR spectra Au and Au−Ni MPC.

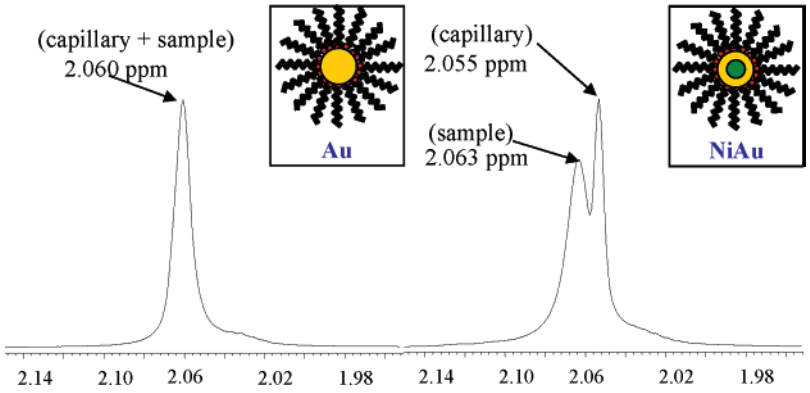


**Figure 10.** Toluene region of the $H^1$ NMR spectra Au and Au−Ni MPC.

of solvent molecules in and out of the magnetic field generated by the nanoparticles. Because this exchange is fast on the NMR time scale, only a single averaged signal is observed.[51]

Figure 10 shows the expanded toluene methyl region for a less concentrated sample, where the peak shift is more easily measured. Under these conditions, eq 1[47,48] can be used to relate the observed peak shift ($\Delta\upsilon$) in the toluene methyl peak to the molar magnetic susceptibility, $\chi_m$, of the NiAu MPCs:

$$\chi_m = 477(\Delta\upsilon)/2\upsilon_1 c + \chi_0 \quad (1)$$

The room-temperature uncorrected magnetic susceptibility of the NiAu MPCs, expressed in terms of the Ni content of the samples, was thereby determined to be 0.0015 $cm^3$/mol of Ni ($25 \times 10^{-6}$ $cm^3/g_{Ni}$). This value is not corrected for the diamagnetic contributions (which are difficult to estimate in this system) and represents the net magnetic susceptibility only.

## Conclusions

A method for preparing magnetic NiAu nanoparticles <5 nm within the bulk miscibility gap was developed. Aqueous $Au^{III}$ and $Ni^{II}$ salts were coreduced in the presence of G5-OH PAMAM dendrimers in 25 mM $NaClO_4$ to form dendrimer-stabilized nanoparticles in water. High concentrations of perchlorate were found to diminish the stability of dendrimer templated nanoparticles, so the particles were extracted into toluene with decanethiol after the reduction step. The resulting

NiAu MPCs were approximately 3 nm in diameter and had essentially the same Au:Ni ratio as was set in the synthesis (Au:Ni = 2.1). UV−vis spectra and control extraction experiments indicated that the particles have surfaces enriched in Au. XPS data indicated that the Ni is likely present as a Ni−NiB mixed material. The magnetic properties of the NiAu MPCs were evaluated with low-temperature SQUID measurements and ambient-temperature Evan's method experiments. At 5 K, the NiAu MPCs had a coercitivity of 60 Oe and a saturation magnetization of approximately 10 emu/g Ni. Their room-temperature magnetic susceptibility, uncorrected for diamagnetic contributions, was determined to be 0.0015 $cm^3/mol_{Ni}$ or $25 \times 10^{-6}$ $cm^3/g_{Ni}$.

**Acknowledgment.** We gratefully acknowledge the Robert A. Welch Foundation (Grant Nos. W-1552 and F-1529) and the U.S. National Science Foundation (Grant No. CHE-0449549) for financial support of our work. B.J.A. thanks the Arnold and Mabel Beckman Foundation for support through the Beckman Scholar program. We also thank Prof. Adam Urbach and Dr. John Gilbertson at Trinity University and Prof. Dick Crooks at the University of Texas at Austin for helpful discussions.

**Supporting Information Available:** UV−visible study results on the effects of ionic strength on the stability of Au DENs, AA data for multiple samples of NiAu MPCs, and UV−visible study results of the stability of NiAu MPCs. This material is available free of charge via the Internet at http://pubs.acs.org.

## References and Notes

(1) Daniel, M.-C.; Astruc, D. *Chem. Rev.* **2004**, *104*, 293−346.
(2) Brust, M.; Kiely, C. J. *Colloids Surf., A* **2002**, *202*, 175−186.
(3) Brust, M.; Walker, M.; Bethell, D.; Schiffrin, D. J.; Whyman, R. *J. Chem. Soc., Chem. Commun.* **1994**, 801−802.
(4) El-Sayed, M. A. *Acc. Chem. Res.* **2004**, *37*, 326−333.
(5) Scott, R. W. J.; Wilson, O. M.; Crooks, R. M. *J. Phys. Chem. B* **2005**, *109*, 692−704.
(6) Bogdanov, A.; Weissleder, R. U.S. Pat. Appl. Publ., 2002; 18 pp.
(7) Perez, J. M.; Simeone, F. J.; Saeki, Y.; Josephson, L.; Weissleder, R. *J. Am. Chem. Soc.* **2003**, *125*, 1019−10193.
(8) Ross, B.; Rehemtulla, A.; Koo, Y.-E. L.; Reddy, R.; Kim, G.; Behrend, C.; Buck, S.; Schneider, R. J.; Philbert, M. A.; Weissleder, R.; Kopelman, R. *Proc. SPIE* **2004**, *5331*.
(9) Stoeva, S. I.; Huo, F.; Lee, J.-S.; Mirkin, C. A. *J. Am. Chem. Soc.* **2005**, *127*, 15362−15363.
(10) Weizmann, Y.; Patolsky, F.; Katz, E.; Willner, I. *J. Am. Chem. Soc.* **2003**, *125*, 3452−3454.
(11) Weizmann, Y.; Patolsky, F.; Katz, E.; Willner, I. *ChemBioChem* **2004**, *5*, 943−948.
(12) Gu, H.; Xu, K.; Xu, C.; Xu, B. *Chem. Commun.* **2006**, 941−949.
(13) Lee, W..; Kim, M. G.; Choi, J..; Park, J.-I.; Ko, S. J.; Oh, S. J.; Cheon, J. *J. Am. Chem. Soc.* **2005**, *127*, 16090−16097.
(14) Love, J. C.; Estroff, L. A.; Kriebel, J. K.; Nuzzo, R. G.; Whitesides, G. M. *Chem. Rev.* **2005**, *105*, 1103−1169.
(15) Urbach, A.; Love, J. C.; Prentiss, M. G.; Whitesides, G. M. *J. Am. Chem. Soc.* **2003**, *125*, 12704−12705.
(16) Knecht, M. R.; Garcia-Martinez, J. C.; Crooks, R. M. *Chem. Mater.* **2006**, *18*, 5039−5044.
(17) Chandler, B. D.; Gilbertson, J. D. In *Topics in Organometallic Chemistry*; Gade, L., Ed.; Springer: Berlin, 2006; Vol. 21, pp 97−120.
(18) Garcia-Martinez, J. C.; Crooks, R. M. *J. Am. Chem. Soc* **2004**, *126*, 16170−16178.
(19) Garcia-Martinez, J. C.; Wilson, O. M.; Scott, R. W. J.; Crooks, R. M. *ACS Symp. Ser.* **2006**, *928*, 215−229.
(20) Kim, Y.-G.; Oh, S.-K.; Crooks, R. M. *Chem. Mater.* **2004**, *16*, 167−172.
(21) Scott, R. W. J.; Wilson, O. M.; Oh, S.-K.; Kenik, E. A.; Crooks, R. M. *J. Am. Chem. Soc.* **2004**, *126*, 15583−15591.
(22) Wilson, O. M.; Scott, R. W. J.; Garcia-Martinez, J. C.; Crooks, R. M. *Chem. Mater.* **2004**, *16*, 4202−4204.
(23) Wilson, O. M.; Scott, R. W. J.; Garcia-Martinez, J. C.; Crooks, R. M. *J. Am. Chem. Soc.* **2005**, *127*, 1015−1024.
(24) Besenbacher, F.; Chorkendorff, I.; Clausen, B. S.; Hammer, B.; Molenbroek, A. M.; Norskov, J. K.; Stensgaard, I. *Science* **1998**, *279*, 1913−1915.
(25) Jones, T. E.; Noakes, T. C. Q.; Bailey, P.; Baddeley, C. J. *J. Phys. Chem. B* **2004**, *108*, 4759−4766.
(26) Jones, T. E.; Noakes, T. C. Q.; Bailey, P.; Baddeley, C. J. *Surf. Sci.* **2006**, *600*, 2129−2137.
(27) Hultgren, R.; Orr, R. L.; Anderson, P. D.; Kelley, K. K. *Selected Values of Thermodynamic Properties of Metals and Alloys*; John Wiley & Sons, Inc.: New York, 1963.
(28) Yuan, G.; Louis, C.; Delannoy, L.; Keane, M. A. *J. Catal.* **2007**, *247*, 256−268.
(29) Chin, Y.-H.; King, D. L.; Roh, H.-S.; Wang, Y.; Heald, S. M. *J. Catal.* **2006**, *244*, 153−162.
(30) Molenbroek, A. M.; Norskov, J. K.; Clausen, B. S. *J. Phys. Chem. B* **2001**, *105*, 5450−5458.
(31) Kim, C. C.; Want, C. H.; Yang, Y. C.; Hwu, Y. K.; Seol, S.; Kwon, Y. B.; Chen, C. H.; Liou, H. W.; Lin, H. M.; Margaritondo, G.; Je, J. H. *Mater. Chem. Phys.* **2006**, *100*, 292−295.
(32) Brayner, R.; Coradin, T.; Vaulay, M.-J.; Mangeney, C.; Livage, J.; Fievet, F. *Colloids Surf., A* **2005**, *256*, 191−197.
(33) Lang, H.; Maldonado, S.; Stevenson, K. J.; Chandler, B. D. *J. Am. Chem. Soc.* **2004**, *126*, 12949−12956.
(34) The brown precipitate was analyzed with AA spectroscopy and determined to primarily consist of Ni and Au, usually with slightly higher Ni:Au ratios than those used in the synthesis. Repeated attempts at solubilizing the material with sonification were unsuccessful. Since the precipitate is generated during the extraction, it likely arises from particle growth and precipitation during that process.
(35) Garcia-Martinez, J. C.; Crooks, R. *J. Am. Chem. Soc.* **2004**, *126*, 16170−16178.
(36) Lang, H.; May, R. A.; Iversen, B. L.; Chandler, B. D. *J. Am. Chem. Soc.* **2003**, *125*, 14832−14836.
(37) Swift, P. *Surf. Interface. Anal.* **1982**, *4*, 47−51.
(38) *Handbook of x-ray photoelectron spectroscopy: a reference book of standard spectra for identification*; Physical Electronics: Eden Prairie, MN, 1995.
(39) Shirley, D. A. *Phys. Rev. B* **1972**, *5*, 4709.
(40) Cotton, F. A. W., G. *Advanced Inorganic Chemistry*, 5th ed.; John Wiley & Sons: New York, 1988.
(41) Knecht, M. R.; Garcia-Martinez, J. C.; Crooks, R. M. *Langmuir* **2005**, *21*, 11981−11986.
(42) Lim, D. C.; Lopex-Salido, I.; Dietsche, R.; Bubk, M.; Dok, Kim, Y. *Angew. Chem., Int. Ed.* **2006**, *45*, 2413−2415.
(43) Negishi, Y.; Nabusada, K.; Tsukuda, T. *J. Am. Chem. Soc.* **2005**, *127*, 5261−5270.
(44) Legrand, J.; Taleb, A.; Gota, S.; Guittet, M.-J.; Petit, C. *Langmuir* **2002**, *18*, 4131−4137.
(45) Averitt, R. D.; Sarkar, D.; Halas, N. J. *Phys. Rev. Lett.* **1997**, *78*, 4217−4220.
(46) Cordente, N.; Respaud, M.; Senocq, F.; Casanove, M. J.; Amiens, C.; Chaudret, B. *Nanoletters* **2001**, *1*, 565.
(47) Evans, D. F. *J. Chem. Soc.* **1959**, 2003−2005.
(48) Sur, S. K. *J. Magn. Reson.* **1989**, *82*, 169−173.
(49) Gottlieb, H. E.; Kotlyar, V.; Nudelman, A. *J. Org. Chem.* **1997**, *62*, 7512−7515.
(50) Purification with a single precipitation resulted in a small observable shift in the toluene methyl peak.
(51) Gatteschi, D.; Sessoli, R.; Villain, J. *Molecular Nanomagnets*; Oxford University Press: New York, 2006.